HIGH RESOLUTION BACKSCATTER ELECTRON (BSE) IMAGING OF IMMUNOGOLD WITH IN-LENS AND BELOW-THE-LENS FIELD EMISSION SCANNING ELECTRON MICROSCOPES

S.L. Erlandsen*, P. T. Macechko and C. Frethem

Dept. of Cell Biology and Neuroanatomy, University of Minnesota School of Medicine, Minneapolis, MN 55455

Abstract

High resolution backscatter electron (BSE) imaging of colloidal gold with field emission scanning electron microscopy (FESEM) depends upon selection of accelerating voltage, beam current, working distance between specimen and backscatter detector, type of backscatter detector, plus the nature and thickness of the metal coating used to improve conductivity and signal collection. BSE imaging of a gold standard (6 nm, 12 nm, and 18 nm colloidal gold) was investigated with in-lens FESEM using a yttrium-aluminum garnet (YAG) scintillator detector and with below-the-lens FESEM using solid state and scintillator detectors, with the former providing the best imaging. Thin metal coatings (<1 nm) of platinum did not interfere with detection of the gold standard with in-lens FESEM so this thickness of platinum was used to test the BSE imaging of 12 nm gold with either solid state or scintillator detectors in below-the-lens FESEM. Due to the thin metal coatings used, a "charging" phenomenon was seen with secondary electron imaging, but this was negligible with BSE imaging because of their higher energy level. Highest BSE resolution was attained on the gold standard and biological samples with in-lens FESEM, but with below-lens FESEM, the labeling of surface molecules with 12 nm immunogold was successfully detected on coated cells at working distances (WD) of 6-20 mm, although shorter WD provided better quality images.

Key Words: High resolution backscatter electron imaging, in-lens field emission scanning electron microscope, below-lens field emission scanning electron microscope, colloidal gold, thin platinum coating.

*Address for correspondence:
Stanley L. Erlandsen
Department of Genetics, Cell Biology and Development
6-160 Jackson Hall
University of Minnesota School of Medicine
Minneapolis, MN 55455, USA
                    Telephone Number: (612)-624-1491
                              FAX Number: (612)-624-8118
                    E-mail: stan@snowman.med.umn.edu

Introduction

In the last decade, the development of field emission scanning electron microscopes (FESEM) equipped with high excitation immersion lenses (in-lens) has led to dramatic improvements in the resolution of surface topography on biological samples, i.e.,on the order of 2-3 nm for periodic structures in infinitely thin samples (Hermann and Müller, 1991) and 4-6 nm on bulk samples (Erlandsen *et al*., 1989, 1990a). Improvements by Autrata (1992) in the design of the yttrium aluminum garnet (YAG) scintillator detector for backscatter electrons (BSE) has permitted the use of low accelerating voltages of <5 kV on biological samples which substantially reduces radiation damage to the specimen (Pawley and Erlandsen, 1989; Pawley, 1992). The Autrata modified YAG detector has also resulted in improved detection of 5-10 nm colloidal gold labels at low accelerating voltages, <5 kV (Autrata, 1992; Olmsted *et al*., 1993; Erlandsen *et al*., 1995) and high resolution detection of <1 nm gold at higher accelerating voltages of 20-30 kV (Hermann *et al*., 1991; Erlandsen *et al*., 1990b). The improved BSE detection of colloidal gold labels and the increased visualization of the surface topography of cellular surfaces by FESEM has greatly facilitated the analysis of cell adhesion molecule distribution on cell surfaces in a number of different cell systems (Hasslen *et al*., 1995; 1996; Olmsted *et al*., 1993; von Andrian *et al*., 1995). The development of the improved YAG detector also has facilitated the use of the double layer coating system for high resolution cryo-FESEM (Walther and Müller, 1997) and has been used to examine the under-surface of resin embedded cells (Richards and ap Gwynn, 1995). Despite providing high resolution of cellular surfaces, one major drawback to the in-lens FESEM has been the limitation on sample size (5-10 mm in X-Y, and ~1-2 mm in Z) due to limited space available in the objective lens (focal length=~2 mm), particularly when a back-scatter electron detector must be fitted in between the objective lens and the specimen.

The design of Schottky electron guns, decelerating systems to obtain low voltage at the specimen, and new "snorkel type" objective lenses has led to the development of new below-the-lens FESEM in which samples approaching inches in diameter may be examined with working distances (WD) ranging from a few to 25-40 mm. Initially

designed in response to demands from the semiconductor industry for the examination of silicon wafers, these new below-the-lens FESEM will facilitate examination of large biological samples such as tissues or animal organs and botanical samples which could never have been accomplished with an in-lens FESEM. Nonetheless, a major concern about below-the-lens FESEM has been whether or not high resolution BSE imaging can be accomplished. Heinzmann *et al*. (1994) used a below-the-lens FESEM with a YAG detector for BSE imaging and reported that 10 nm immunogold particles (marker for epidermal growth factor receptor) could be unambiguously detected at WD of 6-13 mm with accelerating voltages of 3-7 kV on the surfaces of uncoated cells, but that coating the cells with about 1 nm of platinum appeared to mask the BSE signal of the gold particle. Others have also reported that platinum coating of biological samples is not recommended when BSE imaging is to be used to detect colloidal gold of <20 nm (De Harven and Soligo, 1989; Hodges *et al*., 1987; Walther and Müller, 1988).

This paper compares the detection of colloidal gold labels by BSE detection by both in-lens and below-the-lens FESEM. A colloidal gold standard (6 nm, 12 nm, and 18 nm) and samples of human leukocytes were labeled with 12 nm immunogold for surface molecules and were examined in A) an in-lens FESEM equipped with an Autrata modified YAG scintillator detector, and B) four different below-the-lens FESEM using both solid state and scintillator type BSE detectors. Thin platinum coating (about 1 nm), rather than thicker coatings (5-10 nm) were found to give excellent results by improving specimen conductivity to permit BSE detection of the gold signal in all FESEM tested, and this platinum coating did not interfere with BSE imaging of gold at WD of 6-20 mm in these instruments.

Materials and Methods

Colloidal Gold Standard

A gold standard was prepared by mixing 6 nm, 12 nm, and 18 nm colloidal gold (Jackson ImmunoResearch, Inc., West Grove, PA). Glass specimen carriers (5 x 10 mm) prepared from glass slides were treated with 0.1% poly-L-lysine (Sigma Chemical Co., St. Louis, MO) for 1-2 minutes followed by rinsing with distilled water and air drying. The colloidal gold was placed on the glass chips and allowed to adhere for 1-3 minutes before rinsing with distilled water and air drying. The colloidal gold standard was coated by ion beam sputtering with approximately 1 nm of platinum and were examined by FESEM within one week of preparation.

Biological Sample – Cells

Human leukocytes were indirectly immunogold labeled (12 nm) with antibodies specific for the extracellular surface marker CD43, using methods previously described

Figure 1 (*on facing page*). High magnification backscatter electron imaging of 6 nm, 12 nm, and 18 nm colloidal gold. (**A**) Image acquired on Hitachi S-900 in-lens field emission SEM with an "Autrata modified" YAG backscatter electron detector. Arrowheads indicate 6 nm colloidal gold while single arrow shows 12 nm, and double arrow 18 nm colloidal gold. The background consists of a thin film of poly-L-lysine coated with a discontinuous coating of platinum of ~1 nm thickness. Bar equals 60 nm. (**B**) Same sample as in A, but imaged on a below-the-lens field emission SEM at 6 mm WD with a solid state detector. All three colloidal gold sizes seen in A are detected with the solid state detector, but discrimination is less clear and some "ghosting' of image is seen in 6-12 o'clock axis. Bar equals 120 nm. (**C**) Same sample as in A, but imaged on a below-the-lens field emission SEM at 6 mm WD with a Centaurus backscatter electron detector. All three sizes of colloidal gold are imaged with improved clarity over the solid state detector, but with less resolution than that seen in A. "Ghosting" of the gold is seen at an axis of 1-7 o'clock. Bar equals 120 nm.
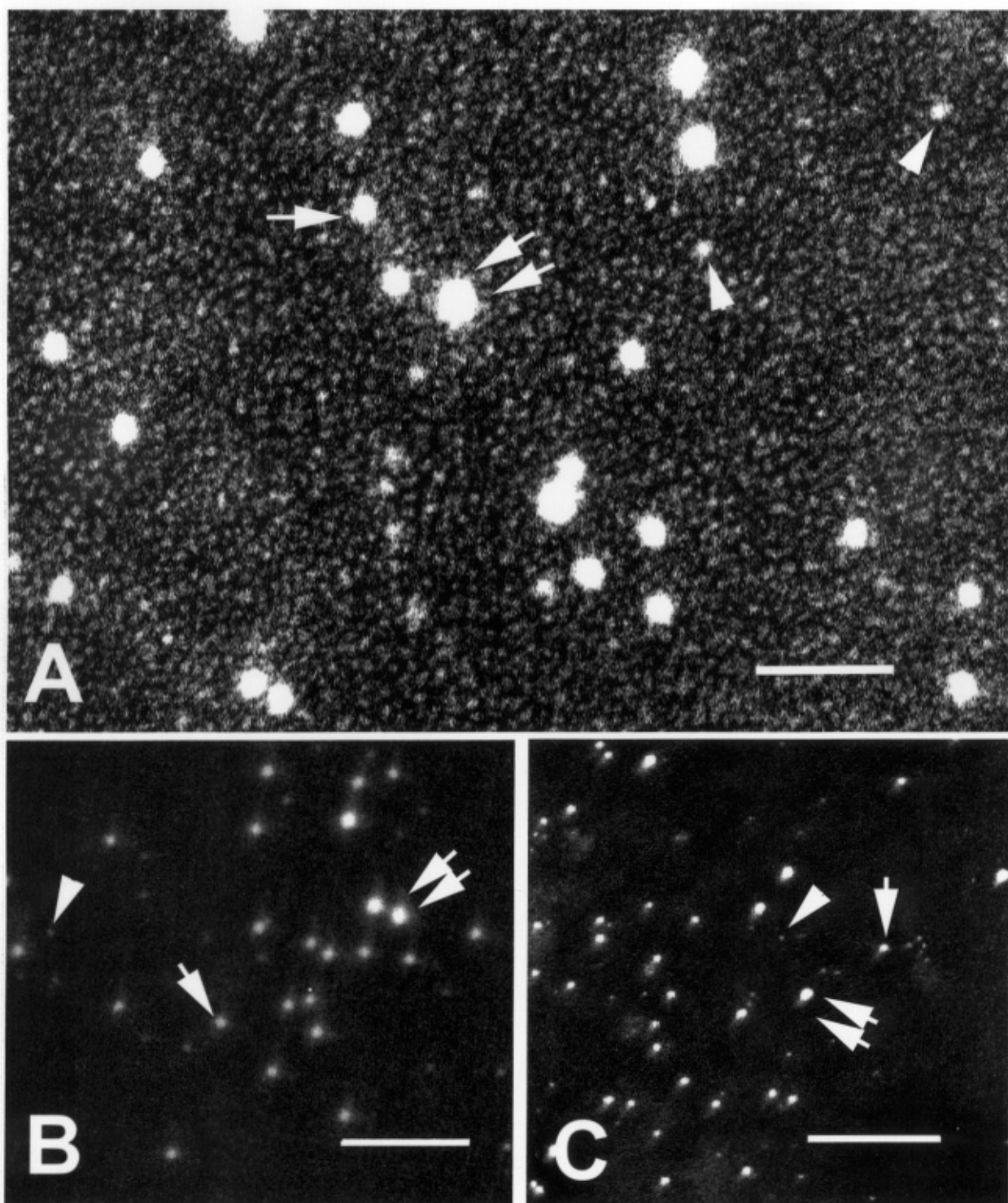

(Erlandsen *et al*., 1993; Hasslen *et al*., 1995; Hasslen *et al*., 1996). Cells were mounted on poly-L-lysine treated glass chips and postfixed in 1% osmium tetroxide for 15 minutes followed by dehydration in ethanol and critical point drying with CO_2. Samples were ion beam coated with approximately 1 nm of platinum and were examined by FESEM within one week of preparation.

Metal Coating

Most samples were coated with approximately 1 nm of platinum by argon ion beam sputtering with a saddle field ion beam gun (VCR Group, Inc., South San Francisco, CA). Planar magnetron sputtering (Balzers MED 010 Device, Liechtenstein) was used to produce platinum coatings of approximally 2 nm, 5 nm, and 10 nm on colloidal gold standards with the coating thickness being measured by a quartz crystal monitor.

In-lens FESEM

All images obtained by in-lens FESEM were acquired with a Hitachi (Tokyo, Japan) S-900 FESEM equipped with an Autrata modified YAG BSE detector with a central conical shaped bore of 1.4-1.5 mm. The threshold for 12 nm colloidal gold in our in-lens FESEM is 1.7 kV; therefore, to obtain a direct comparison under low voltage conditions of the performance of in-lens and below-the-lens FESEM, an accelerating voltage of 5 kV was selected. Also, 5 kV was selected because less radiation damage is produced under low voltage conditions (Pawley, 1992), and it was anticipated that the sensitivity of other BSE detectors would be somewhat less than that of the Autrata modified YAG BSE detector.

Below-the-lens FESEM

Four different below-the-lens FESEM were tested with the gold standard and biological cell sample including: 1) Hitachi S-4700 FESEM (Nissei Sangyo America, Ltd., Sunnyvale, CA); 2) JEOL 6340F FESEM (JEOL USA, Peabody, MA); 3) LEO 1500 FESEM (LEO Electron Microscopy Inc., Thornwood, NY); and 4) Philips S XL30 FESEM (Philips Electronic Instruments Co., Chicago, IL). All instruments were tested in applications laboratories and company operators optimized performance of each micro-
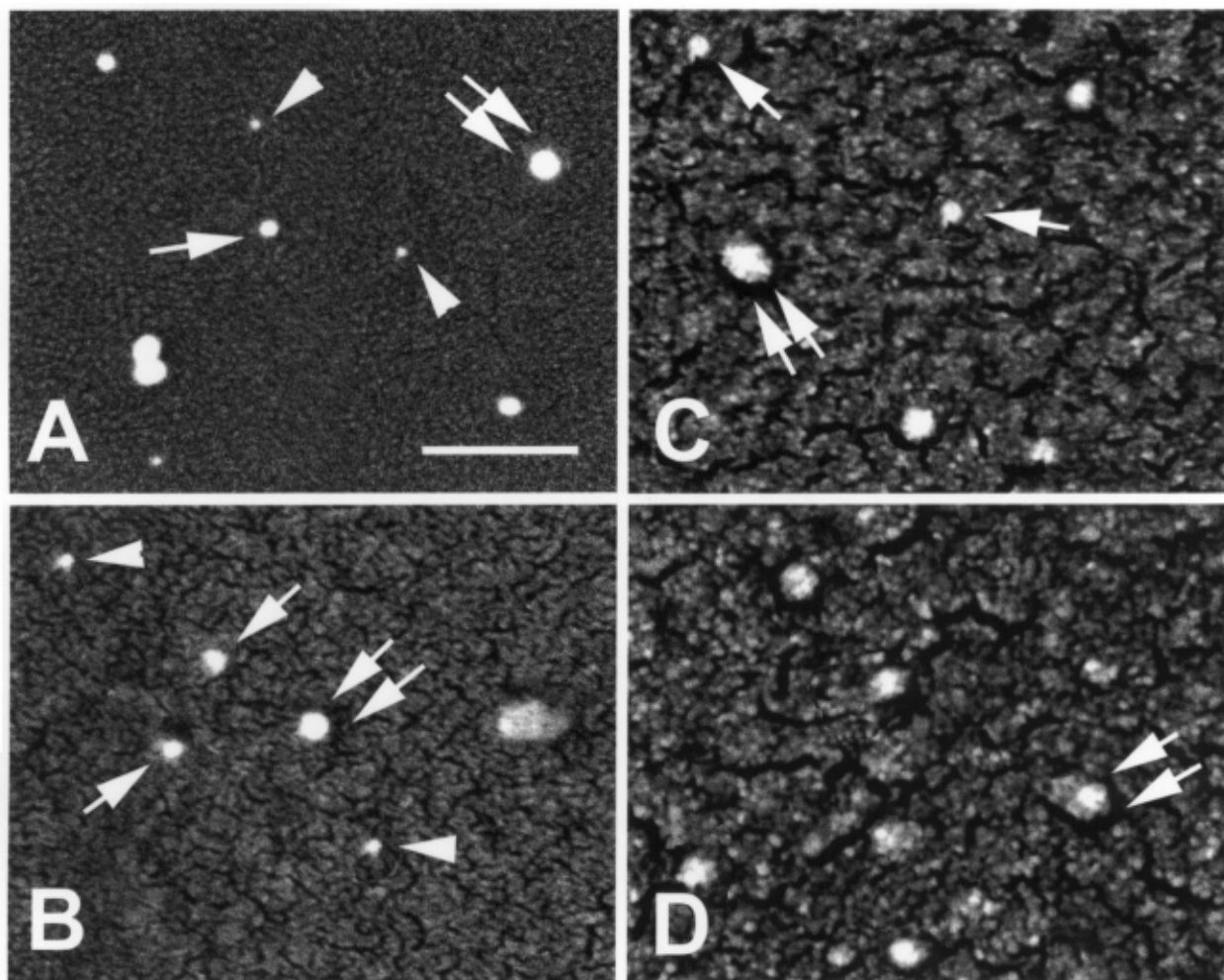
Figure 2. High resolution backscatter electron image of colloidal gold standard (6 nm, 12 nm, and 18 nm) acquired with a modified "Autrata" YAG detector in an Hitachi S-900 in-lens field emission SEM. The effect of different thicknesses of platinum coating on the detection of 6 nm (arrowhead), 12 nm (single arrow), and 18 nm (double arrows) colloidal gold can be clearly seen. (**A**) ~ 1 nm of platinum, saddle field gun ion beam sputtering; (**B-D**), samples were sputter coated at ambient temperature with platinum in a Balzers MED 010 device at a thickness of ~2 nm (**B**), ~5 nm (**C**), and ~10 nm (**D**) as measured by deposition on a crystal monitor. Bar in A equals 120 nm for all panels.

scope. Backscatter electron detectors tested included solid state detectors and a proprietary phosphorus scintillator (Centaurus detector, K.E. Developments Ltd, Cambridge, UK).

Results

The BSE examination of the colloidal gold standard was carried out at the optimum WD for each FESEM. For the in-lens FESEM the WD was fixed at approximately 2 mm for the objective lens, but the distance to the YAG detector is somewhat less since the detector is inserted into

the space between the specimen rod and the objective lens. The shortest WD for below-the-lens FESEM was in the order of 6 mm, but the exact distance between the specimen and the surface of the BSE detector was impossible to determine accurately. Therefore, using below-the-lens FESEM, it was impossible to make direct comparisons between detectors under the conditions of testing, and images shown here are meant to be representative for each detector. BSE imaging of the gold standard with the in-lens FESEM provided the "standard" for comparison with BSE imaging with below-the-lens FESEM, and for both types of microscopes, images were collected at a primary magnifi-
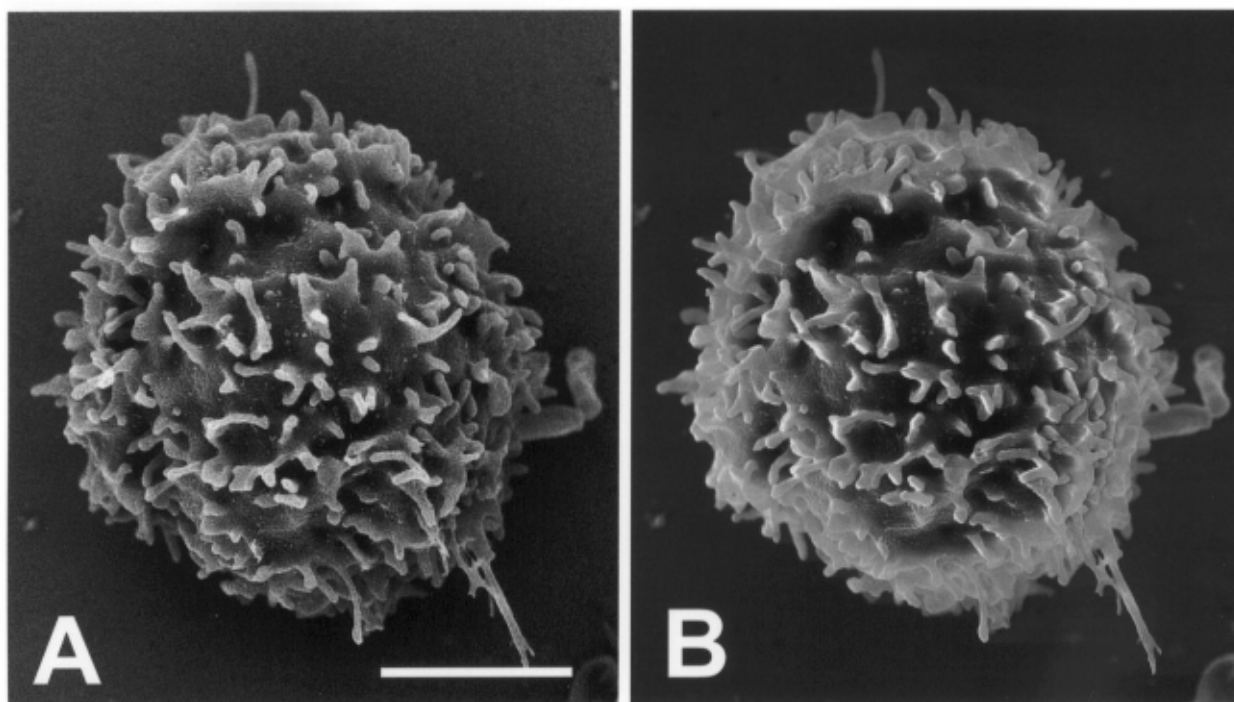
Figure 3. Backscatter electron (**A**) and secondary electron (**B**) imaging of a human lymphocyte immunolabeled for CD43 with 12 nm gold and coated with ~1 nm of platinum by ion beam sputtering. Excessive charging interferes with secondary electron imaging (B), while no charging occurs in the backscatter electron image (A). In the lattter, the 12 nm colloidal gold marker for CD43 can be seen on the cell body of the lymphocyte. Bar in A equals 2 nm.

cation of 250000 X. A high magnification in-lens FESEM BSE image of 6, 12, and 18 nm colloidal gold is shown in Figure 1A while below-the-lens BSE images with a solid state detector and a Centaurus scintillator detector are seen in Figures 1B and 1C, respectively. As expected, the superior imaging capabilities of the in-lens FESEM together with the use of the Autrata modified YAG BSE detector permitted clear and distinct identification of the different sizes of colloidal gold, and also provided a crisp image of the platinum coating in the background (Figure 1A). In below-the-lens FESEM both the solid state and the Centaurus scintillator detector provided detection of the three different sizes of colloidal gold, but the image quality was less than that obtained with the YAG detector and in-lens FESEM (compare Figures 1B and 1C with 1A) and background structure was almost lacking. Some "ghosting" or unidirectional halos of the BSE image of colloidal gold were detected in below-the-lens FESEM with both the use of solid state detector (Figure 1B; cold field gun - FESEM) and a Centaurus detector (Figure 1C; Schottky gun - FESEM).

Application of different thicknesses of metal coating to improve conductive properties of the sample (Figure 2A-D) revealed that the quality of BSE imaging of small sizes

of colloidal gold using in-lens FESEM was inversely proportional to the thickness of the platinum coating. Ion beam sputtering of platinum produced thin discontinuous coatings of less than 1 nm, which did not interfere with detection and discrimination of 6-12 nm colloidal gold by in-lens FESEM (Figure 2A) and similar results were obtained with planar magnetron sputtering of ~2 nm platinum (Figure 2B). Coating colloidal gold standard samples with ~5 nm of platinum obscured the detection of 6 nm gold and when ~10 nm of platinum was used as a coating it was difficult to discriminate 12 and 18 nm gold even with the Autrata modified YAG detector in the in-lens FESEM. The 1 nm platinum coating achieved with ion beam sputtering was used to coat biological samples and "charging" in BSE imaging was greatly minimized since at an acceleratingvoltage (V_0) of 5 kV, the higher energy of the BSE (~4 kV) negated any effect of the small electrostatic fields present (Figure 3A). However, due to the thousand-fold lower energy level of secondary electrons (SE) (~5 eV), the same small electrostatic fields directly affected the imaging by producing the "charging" phenonemon seen in SE images of the same cell (Figure 3B).
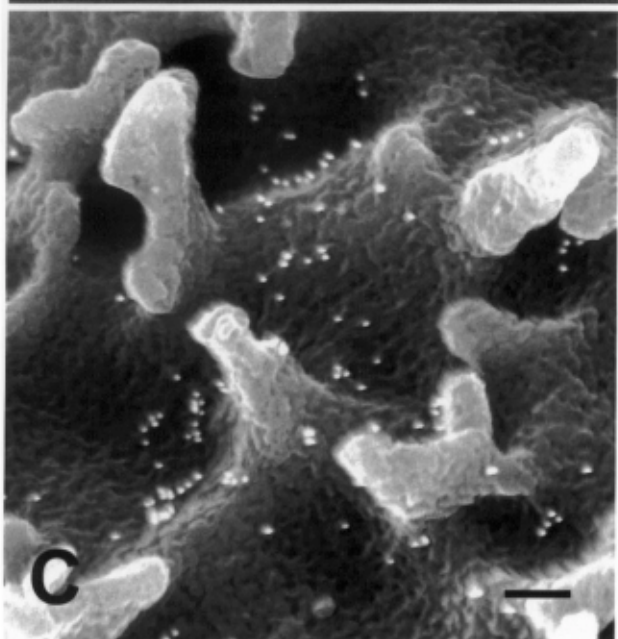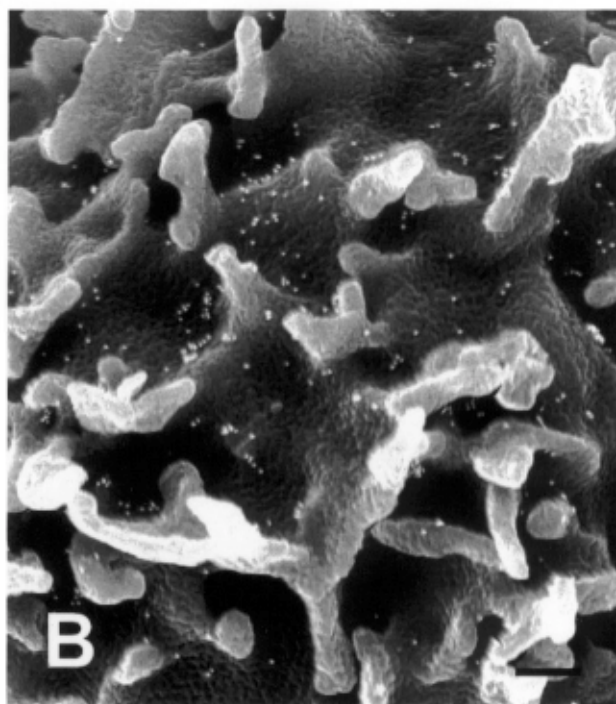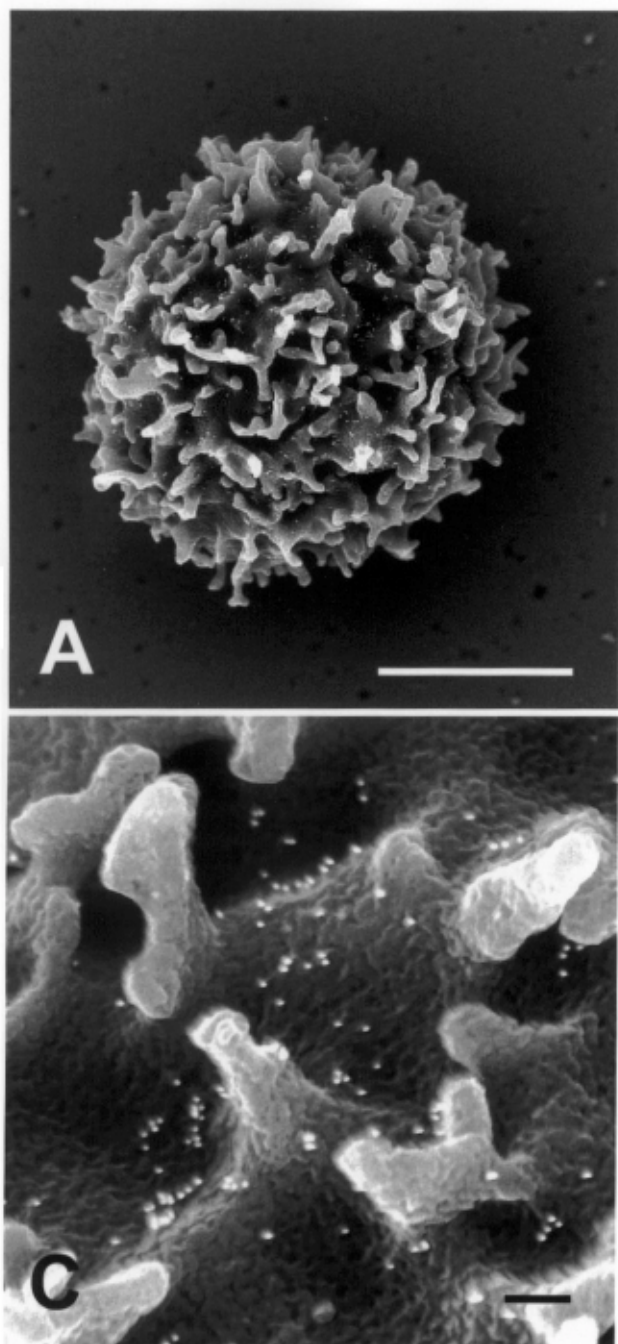
To compare the BSE imaging of biological samples

Figure 4. Human lymphocyte immunogold labeled for CD43 antigen and imaged with modified "Autrata" YAG backscatter electron detector in Hitachi S-900 in-lens field emission SEM. (**A**) At initial magnification of 15000 X, single and clusters of 12 nm colloidal gold particles can be identified on the surface of the leukocyte. Bar equals 2 mm. (**B**) At a magnification of 50000 X, clusters of immunogold particles (seen as white spheres) can be easily detected on the cell body. Bar equals 100 nm. (**C**) Image acquired at 100000 X sharply defines clusters of gold particles permitting identification of single particles. Bar equals 60 nm.

with in-lens and below-the-lens FESEM, a test sample was chosen consisting of human leukocytes that were indirectly immunogold labeled with 12 nm colloidal gold. BSE images were taken at low magnifications (8000-15000 X) and at a higher magnification (50000 X) that would permit identification of the colloidal gold particle. Using in-lens FESEM with a YAG BSE detector, it was possible to clearly visualize the 12 nm colloidal immunogold particles at low magnification (Figure 4A) and easily discern clusters of colloidal gold particles at higher magnifications (Figures

4B and 4C). Examination of similar immunogold labeled leukocytes in below-the-lens FESEM was performed at accelerating voltages of 3-5 kV and at different WD. An accelerating voltage of 5 kV was chosen for comparison of microscopes to favor the greater collection of BSE and the use of a smaller probe, but the use of 3 kV also produced good quality BSE images of colloidal gold in each below-the-lens FESEM tested, although the overall image quality was not quite as sharp as that of the same image taken at 5 kV (compare Figures 5A and 5B). Similarly, each below-the-lens instrument had an optimal WD for BSE imaging for each BSE detector, but despite this, the BSE imaging of colloidal gold particles was seen to be excellent at 6-16 mm of WD in all instruments tested (Figures 6, 7, 8), although a higher overall quality of imaging was obtained at shorter WD. Colloidal gold on leukocyte surfaces was de-
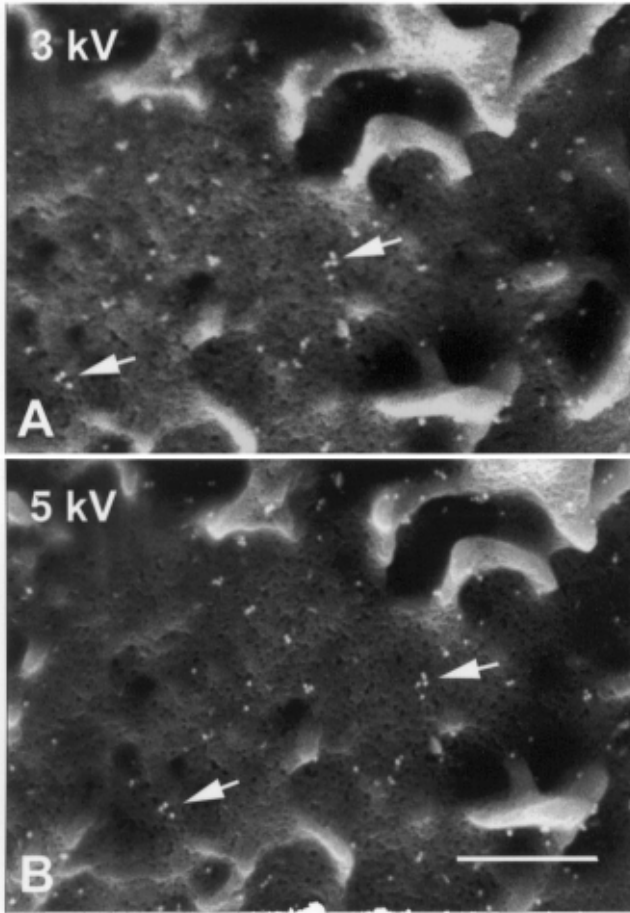
Figure 5. Effect of accelerating voltage on the backscatter electron imaging (solid state detector) of colloidal immunogold staining on a human leukocyte in a below-the-lens field emission SEM at 6 mm WD. By comparing the same clusters of 12 nm colloidal gold particles seen at the arrows in panels (**A**) and (**B**), the detection of the gold particles in A at 3 kV can be seen to be less distinct than the same particles seen at 5 kV in B. Bar equals 500 nm.

Figure 6. Effect of WD on the backscatter electron imaging (solid state detector) of colloidal immunogold staining on a human leukocyte in a below-the-lens field emission SEM. Short WD of 6 mm provided high resolution imaging of gold clusters, but at increased WD of 16 mm there was a small but perceptible loss in imaging quality. Bar equals 500 nm.

tected at 20 mm WD in one instrument (data not shown), but this WD was not tested in every instrument. On occasion, BSE images taken at WD of >14 mm appeared to have colloidal gold particles of slightly larger diameter than those imaged at shorter WD, and it seemed as if magnification might have varied as a result of substantial change to longer WD (see Figures 7D and 8C).

Discussion

Optimal visual definition of the colloidal gold standard (6, 12, and 18 nm particles) was obtained with in-lens FESEM using an Autrata modified YAG BSE detector. This
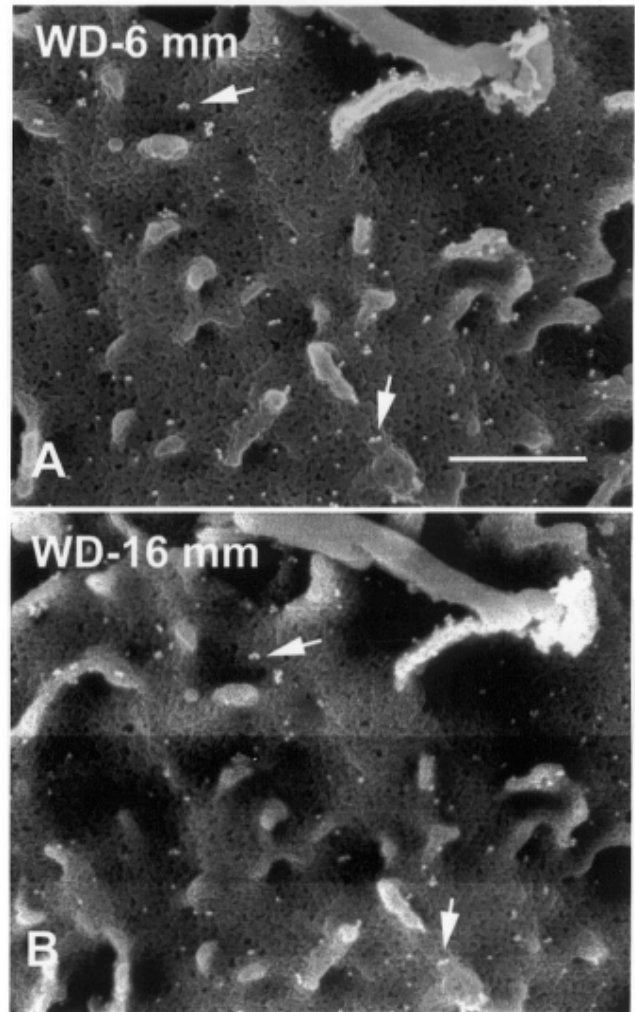
is not unexpected since BSE imaging has been shown by Joy (1991) to provide better resolution and higher contrast of 10 nm colloidal gold than secondary electron imaging. Also, the shorter focal length of the in-lens FESEM together with its better correction for chromatic and spherical aberration permit production of a smaller probe size than can be obtained with below-the-lens FESEM. Nonetheless, using below-the-lens FESEM it was still possible to detect the presence of the three sizes of colloidal gold, including the detection of 6 nm gold although the image quality was greatly reduced in comparison to in-lens FESEM (Figure 1A-C). BSE imaging of colloidal gold coated with 1 nm of
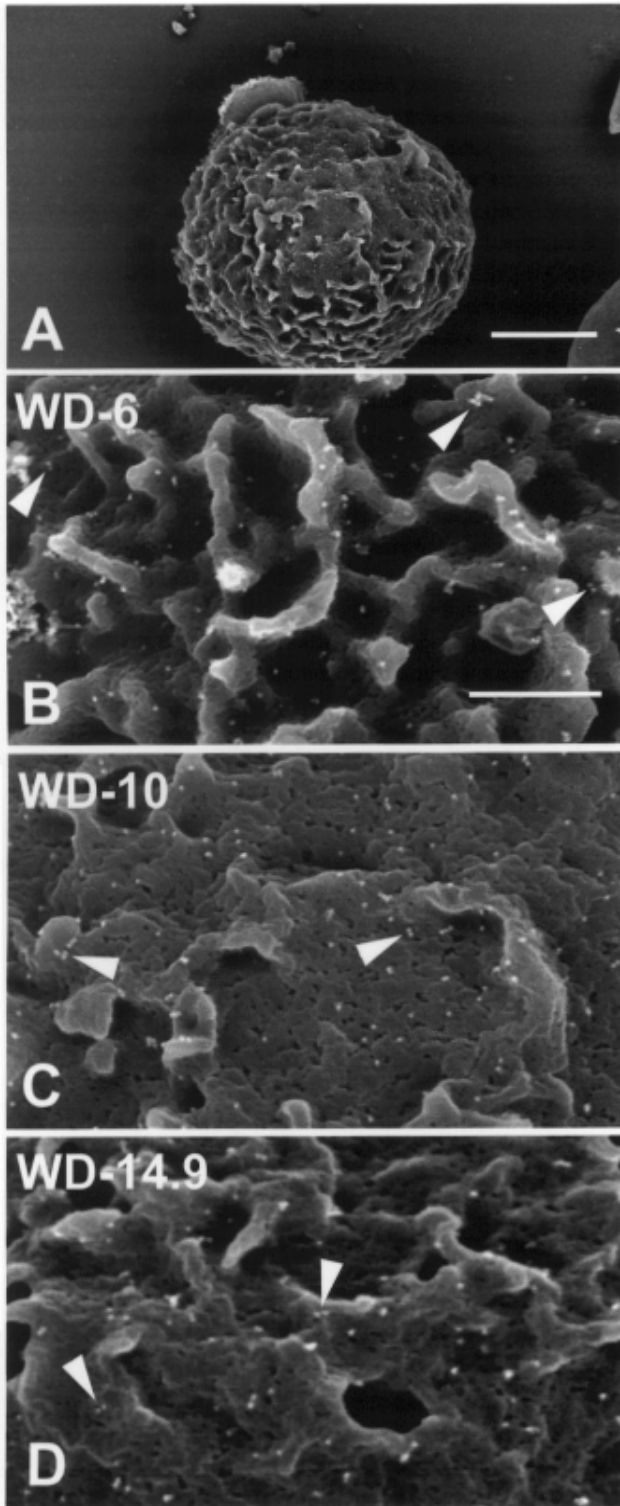
Figure 7 (*at left*). Detection of 12 nm colloidal immunogold particles in a below-the-lens field emission SEM using a solid state backscatter electron detector. The 12 nm gold particles can be detected on the surface of a human leukocyte at low magnification (initially 15000 X at 6 mm WD as shown in (**A**) and are easily resolved at higher magnification (50000 X) as seen in (**B**). Arrowheads indicate multimers of gold particles in B-D. As the WD increases to 10 mm in (**C**), the clarity of the gold particles seems to change little, however, when the WD is changed to 14.9 mm in (**D**), the gold particles seem to vary in both dimension and edge sharpness. A: bar equals 2 mm; B-D: bar equals 500 nm.

contrast) while providing sufficient conductivity to minimize any "charging" effects on the higher energy BSE (80-90% of V_o). However, charging was not eliminated as the less energetic secondary electrons (~5 eV) were effected by "charging" under conditions where BSE imaging was unaffected. Ideally the thin 1 nm platinum coating is compatible with high spatial resolution by BSE at low kV and would not be expected to mask or obscure surface features, such as would be expected with 5-10 nm or thicker coatings of metal (Pawley, 1992).

A surprising finding was that all of the below-the-lens FESEM tested were able to produce excellent images of 12 nm colloidal gold on the surfaces of immunogold labeled cell surfaces that had been coated with a thin 1 nm layer of platinum. Heinzmann *et al*. (1994) had reported that detection of the epidermal growth factor receptor on A431 cells (human epidermoid carcinoma) using 10 nm immunogold was best performed by using a combination of secondary electron signals and BSE signals from uncoated samples. In their work, the surface topography of cell surfaces, consisting of numerous microvilli projecting from the cell surface, was revealed by the secondary electron signal while the BSE signal was used to identify gold particles by material or atomic number contrast, and in some instances also to provide some information on topography. These authors found that coating their biological samples with a thin 1 or 4 nm coating of platinum obscured the detection of 10 nm gold particles. Our results with below-the-lens FESEM clearly shows that both topographical and atomic number contrast (detection of 12 nm gold) can be easily accomplished at WD of 6-20 mm at an accelerating voltage of 5 kV. The surface topography of the A431 cells studied by Heinzmann *et al*. (1994) and the leukocytes in our study were not dissimilar as both possessed numerous microvilli, and the discrepancies between our results and those of Heinzmann can most likely be explained by a culmination of other factors. First, the Autrata YAG detector used by Heinzmann *et al*. (1994) with a below-the-lens FESEM was designed for collection of BSE channeling

platinum was successfully accomplished with both in-lens and below-the-lens FESEM, although thicker layers of 5-10 nm obscured the BSE signal. On biological samples (immunogold labeled human leukocytes) the thin 1 nm platinum coating gave rise to increased signal (topographical
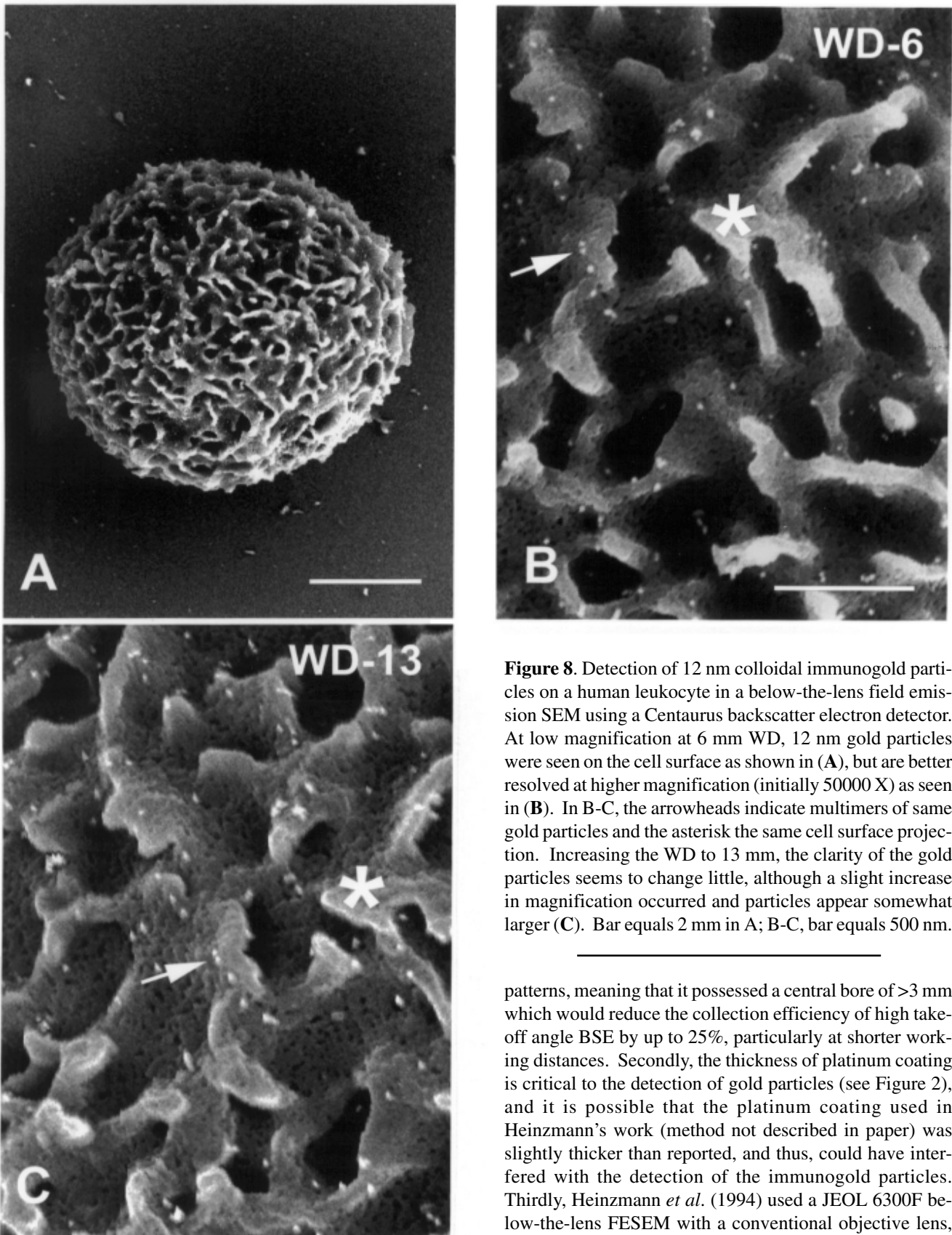
Figure 8. Detection of 12 nm colloidal immunogold particles on a human leukocyte in a below-the-lens field emission SEM using a Centaurus backscatter electron detector. At low magnification at 6 mm WD, 12 nm gold particles were seen on the cell surface as shown in (**A**), but are better resolved at higher magnification (initially 50000 X) as seen in (**B**). In B-C, the arrowheads indicate multimers of same gold particles and the asterisk the same cell surface projection. Increasing the WD to 13 mm, the clarity of the gold particles seems to change little, although a slight increase in magnification occurred and particles appear somewhat larger (**C**). Bar equals 2 mm in A; B-C, bar equals 500 nm.

patterns, meaning that it possessed a central bore of >3 mm which would reduce the collection efficiency of high take-off angle BSE by up to 25%, particularly at shorter working distances. Secondly, the thickness of platinum coating is critical to the detection of gold particles (see Figure 2), and it is possible that the platinum coating used in Heinzmann's work (method not described in paper) was slightly thicker than reported, and thus, could have interfered with the detection of the immunogold particles. Thirdly, Heinzmann *et al*. (1994) used a JEOL 6300F below-the-lens FESEM with a conventional objective lens, whereas, the JEOL 6340F below-the-lens FESEM tested in

51

this report had the new inverted objective lens design. In our hands, this latter instrument easily detected 12 nm immunogold on the surface of leukocytes that had been coated with a thin 1 nm layer of platinum. All together, these three factors (BSE collector efficiency, platinum thickness, and objective lens design) may explain why Heinzmann *et al.* (1994) were unable to visualize 10 nm gold particles in thin platinum coated samples.

Due to differences in the design and location of the BSE detectors in below-the-lens FESEM tested, it was not possible to make direct comparisons with one another. Careful examination of the detection of 12 nm immunogold labeling on leukocytes in this study clearly demonstrates that successful detection of immunogold was accomplished with solid state and phosphor-based scintillator type (Centaurus) BSE detectors. The Centaurus BSE detector appeared to produce slightly better images of the three sizes of colloidal gold (6, 12, and 18 nm) at high magnification, yet it should be pointed out that this conclusion is at best tenuous since both types of detectors were not tested on the same instrument, and other factors may be responsible for the slight differences observed. Both solid state and phosphor based scintillator detectors provided excellent BSE images of 12 nm colloidal gold at magnifications used for most biological work (<50000 X), yet if high resolution BSE imaging was to be performed then the YAG scintillator provided the greatest sensitivity, but at a two-fold higher cost factor.

Chromatic aberration is a dominant factor in regulating the size and profile of the electron probe in low voltage FESEM (Joy, 1987) and can explain two phenomena observed in this investigation. First, the presence of "ghosting" or haloes of the colloidal gold seen with below-the-lens FESEM might be explained by the higher level of chromatic aberration which could result in a wider skirt of electrons when the electron beam is focused on the specimen. The asymmetry of the probe produced by the wider skirt could easily reduce the high resolution signal component in the center of the probe, resulting in less contrast detail and a noisier image, and also could likely produce the "ghost" or halo of the gold particle in the direction of the skirt asymmetry. Secondly, chromatic aberration is also known to produce an image where the size of the colloidal gold is increased in size when acceleration voltage was reduced below 8 kV, a phenomenon referred to as "larger than life" by Hermann and Müller (1991). Joy (1987) has shown that an electron probe in FESEM which is Gaussian at 30 kV will possess a full-width half maximum of about 6 Å, but that a reduction in voltage to 3 kV can increase the diameter of the probe by a factor of two, and more importantly will also change the intensity profile of the probe (widening the skirt), thereby reducing image contrast and worsening resolution. Thus, reducing the accelerating volt-

age from 5 kV to 3 kV (Figure 5) or increasing the WD from 6 mm to >13 mm (Figures 6, 7 and 8) will adversely affect the diameter of the electron probe and worsen the resolution of the image.

In conclusion, BSE detection in below-the-lens FESEM of biological samples coated with a thin layer of platinum (~1-2 nm) provided both excellent topographical contrast of cellular surfaces and detection of 12 nm colloidal gold by atomic number contrast. All four below-the-lens FESEM tested produced excellent BSE images of 12 nm gold with either solid state or scintillator type detectors at routine magnifications up to 50000 X. A comparison of in-lens and below-the-lens FESEM demonstrated that high resolution BSE imaging of immunogold particles (6, 12, and 18 nm) was better accomplished with the former, while the latter had the distinct advantage of variable WD (6-20 mm) which should facilitate the detection and analysis of colloidal gold probes (>10 nm) by BSE imaging on large biological samples.

References

Autrata R (1992) Single crystal detector suitable for high resolution scanning electron microscopy. EMSA Bull **22**: 54-58.

De Harven E, Soligo D (1989) Backscatter electron imaging of the colloidal gold marker on cell surfaces. In: Colloidal Gold, Vol. 1 (Hayat MA, ed). Academic Press, New York, pp. 229-249.

Erlandsen SL, Bemrick WJ, Pawley J (1989) High resolution electron microscopic evidence for the filamentous structure of the cyst wall in *Giardia muris* and *Giardia duodenalis*. J Parasitol **75**: 787-797.

Erlandsen SL, Bemrick WJ, Schupp DE, Shields JM, Jarroll EL, Sauch JF, Pawley JB (1990a) High resolution immunogold localization of *Giardia* cyst wall antigens using field emission SEM with secondary and backscatter electron imaging. J Histochem Cytochem **38**: 625-632.

Erlandsen SL, C Frethem C, Autrata R (1990b) Workshop on high-resolution immunocytochemistry of cell surfaces using field emission SEM. J Histochem Cytochem **38**: 1779-1780.

Erlandsen SL, Hasslen SR, Nelson RD (1993) Detec-

tion and spatial distribution of the B$_2$ integrin (Mac-1) and L-selectin (LECAM-1) adherence receptors on human neutrophils using high resolution field emission SEM. J Histochem Cytochem **41**: 327-333.

Erlandsen SL, Nelson RD, Hasslen SR, Dunny GM, Olmsted SB, Frethem C, Wells CL (1995) High resolution FESEM: Application of backscatter electron (BSE) imaging for biological samples. Workshop on Ultra High Resolution SEM, Oak Ridge National Lab and Univ Tennessee. Joy D (ed). Hitachi Instrument News **27**: 10-15.

Hasslen SH, von Andrian UH, Butcher EC, Nelson RD, Erlandsen SL (1995) Spatial distribution of L-selectin (CD62L) on human lymphocytes and transfected murine L1-2 cells. Histochem J **27**: 547-554.

Hasslen SR, Burns AR, Smith CW, Starr K, Barclay AN, Michie SA, Nelson RD, Erlandsen SL (1996) Preservation of leukocyte surface molecules by aldehyde fixation: flow cytometry and high resolution FESEM studies of CD62L, CD11b, and Thy-1. J Histochem Cytochem **44**: 1115-1122.

Heinzman U, Reininger A, Autrata R, Höfler H (1994) Imaging of immunolabeled membrane receptors in uncoated SEM specimens. Scanning **16**: 241-245.

Hermann R, Schwartz H, Müller M (1991) High precision immuno-scanning electron microscopy using fab fragments coupled to ultra-small colloidal gold. J Struct Biol **107**: 38-47.

Hermann R, Müller M (1991) Prerequisites of high resolution scanning electron microscopy. Scanning Microsc **5**: 653-664.

Hodges GM, Southgate J, Toulson EC (1987) Colloidal gold - a powerful tool in scanning electron microscope immunocytochemistry: an overview of bioapplications. Scanning Microsc **1**: 301-318.

Joy DC (1987) Low voltage scanning electron microscopy. Inst Phys Conf Ser **90**: 175-180.

Joy DC (1991) Contrast in high-resolution scanning electron microscope images. J Microsc **161**: 343-355.

Olmstead SB, Erlandsen SL, Dunny GM, Wells CL (1993) High-resolution visualization by field emission scanning electron microscopy of *Enterococcus faecalis* cell surface proteins encoded by the pheromone-induced conjugative plasmid pCF10. J Bacteriol **175**: 6229-6237.

Pawley JB, Erlandsen SL (1989) The case for low voltage high resolution scanning electron microscopy of biological samples. In: The Science of Biological Specimen Preparation for Microscopy and Microanalysis 1988. Albrecht RM and Ornberg RL (eds). Scanning Microscopy International, Chicago, IL. pp. 163-173.

Pawley JB (1992) LVSEM for high resolution topographic and density contrast imaging. In: Advances in Electronic Electron Physics, vol. 83. Hawkes PW, Kazan B (eds). Academic Press, New York. pp. 203-274.

Richards RG, ap Gwynn I (1995) Backscatter electron imaging of the undersurface of resin-embedded cells by field emission scanning electron microscopy. J Microsc **177**: 43-52.

Von Andrian UH, Hasslen SR, Nelson RD, Erlandsen SL, Butcher EC (1995) A central role for microvillous receptor presentation in leukocyte adhesion under flow. Cell **82**: 1-20.

Walther P, Müller M (1988) Detection of small (5-15 nm) gold-labeled surface antigens using backscattered electons. In Biotechnology and Bioapplications of Colloidal Gold (Albrecht RM, Hodges GM (eds). Scanning Microscopy International, Chicago, IL. pp. 63-70.

Walther P, Müller M (1997) Double-layer coating for field emission cryo-scanning eletron microscopy - present state and applications. Scanning **19**: 343-348.

Discussion with Reviewers

G.M. Roomans: Among the below-the-lens instruments that you tested, two have a cold field emission gun, and two have a thermal, Schottky-type gun. The former gun type is supposed to provide better resolution (albeit at the cost of some inconvenience). However, you did not mention a difference in the performance of the four below-the-lens instruments. Could you comment on this?

Authors: Indeed, the in-lens cold field emission SEM provides better BSE resolution than any of the below-the-lens FESEM instruments and this can clearly be seen by examination of BSE imaging of different sizes of colloidal gold and background structure as shown in Figure 1. There is very little inconvenience of the in-lens FESEM, as compared to the below-the-lens FESEM instruments, unless one refers to either the restriction on sample size with best results being achieved with small samples, i.e., single cells or suspensions, or perhaps the need to flash the cold field emitter at the beginning of each day, but both of these are minor points between these two instrument types. Examination of human leukocytes labeled with 12 nm immunogold revealed similar results in BSE imaging with all four below-the-lens FESEM instruments, despite the fact that different BSE detectors were used on these instruments (minor differences occurred in imaging at long working distances, but was related to differences in BSE detectors). The comparison of BSE imaging was made on biological samples with photos of immunogold being taken at 50000 X, the conditions in which we anticipated the greatest usage in our laboratory, and although this parameter was not designed to test for differences in resolution, we were pleasantly surprised by the excellent performance of all instruments using this criteria. Another factor prohibiting comparisons of resolution was the inability to use the same BSE detector on the all four of these FESEM instruments.

R.G. Richards: A slightly fairer comparison of below-the-lens and in-lens FESEM instruments would be to use a YAG detector in both cases. Where there YAG detectors available for the below-the-lens FESEM instruments?

Authors: For several reasons including availability, it was not possible to test YAG detectors for BSE imaging on all four below-the-lens FESEMs. In one case, the YAG detector was not installed due to damage during shipping and in another case, it was not the appropriate YAG crystal size. It would have been very desirable to make this comparison with the same detector, but the expensive cost of the YAG detector prohibited several manufacturers from having them available. We have purchased a YAG detector for our new below-the-lens FESEM and will make the comparisons you asked for with our in-lens FESEM, and we hope to report on this in the next year.

R.G. Richards: Did you look at uncoated specimens and if so, what were the effects of charging on the SE and BSE image? Did you try carbon coating and did this increase or decrease the signal of the gold with BSE imaging? What were the effects of charging on the image?

Authors: For BSE imaging, we did not look at uncoated specimens because we find that a thin coating of platinum (~1 nm) is optimum in our hands for minimizing the "charging" phenomenon due to small electrostatic fields in the sample. In Figure 3A and 3B, we demonstrated that BSE imaging is relatively unaffected by small electrical fields while SE imaging is grossly distorted, and this is due to the difference in energy for BSE (~4 kV) and SE (~5 eV). Also, we have not tried carbon coating for the reason stated above.

R.G. Richards: In your comparison of different coating thickness you used ion beam sputtering for 1 nm and planar magnetron sputtering for the thicker coatings. What were thicker coatings like with the ion beam sputtering and was it possible to coat 1 nm with the planar magnetron? Vacuum pumping times, the type of pump, the amount of cooling of the head, and of cold trap cooling with liquid nitrogen fingers all play a part in the quality of the coating. Were these optimized?

Authors: We did not try thicker coatings with the ion beam because the deposit ion rate with our machine requires 6-7 minutes to obtain an approximately 1 nm coating, and while we have empirically determined the time required for this thickness, we do not have a quartz crystal monitor to gauge thicker coatings. Instead, for thicker coatings we used planar magnetron sputtering to make 2, 5, and 10 nm thick Pt coatings as determined by a quartz crystal monitor. The Ion Beam Coating was carried out in a Denton (Moorestown, NJ) Evaporator with a 5" oil diffusion pump (Santovac 5 oil [polymethyl ether to minimize backstreaming], Electron Microscopy Science, Fort Washington, PA) whereas the Balzers (Liechtenstein) MED device uses a turbo pump for vacuum production. Pt coating was carried out at ambient temperature in both systems. In both cases, the procedures for coating was optimized. Examination of Figure 2 clearly shows the difference between ion beam sputtering and planar magnetron sputtering as imaged by an in-lens FESEM.